Journal of
Marine Science and Engineering

MDPI

Article

Morphology and Effect of Load on Bridge Piers Impacted by Continuous Sea Ice

Li Gong [1,2], Yue Cui [1,*], Yunfei Du [1], Long Qin [1] and Xinyuan Zhao [1]

[1] Department of Civil Engineering, Lanzhou Jiaotong University, Lanzhou 730070, China; gongl@mail.lzjtu.cn (L.G.); dyf980521@163.com (Y.D.); ql227790@163.com (L.Q.); 15294124865@163.com (X.Z.)
[2] Gansu Normal University for Nationalities, Gannan Tibetan Autonomous Prefecture, Hezuo 747000, China
* Correspondence: cy17393182939@163.com

Abstract: In order to study the collision of sea ice on bridge piers of a sea-crossing bridge, this study establishes a finite element model of the impact of sea ice on bridge piers in aqueous media based on explicit dynamics analysis software and programming software using the arbitrary Lagrangian Eulerian (ALE) method. The results show that, when the sea-ice spacing is larger than the sea-ice edge length, the increase in sea-ice spacing leads to a decrease in the collision force and a significant increase in the probability of climbing and overturning. The increase in sea-ice mass significantly increases the impact force on the bridge abutment, and the peak value increases linearly with the increase in mass, and the sea-ice climbing and overturning phenomena are obvious. Different shapes of sea ice are obtained by cutting the sea-ice field with the two-dimensional Voronoi method, and the maximum impact force increases significantly with the increase in the average area. Irregularly shaped sea ice leads to a larger impact force and triggers the accumulation climbing phenomenon, which is verified by experiments, and the experimental values are in good agreement with the simulated values. In conclusion, this study reveals the significant effects of the spacing, mass, and shape of sea ice on the impact force of bridge piers, which provides an important reference for the design of bridge structures.

Keywords: numerical simulation; sea ice; ice load; impact of successive impacts; ice size

Citation: Gong, L.; Cui, Y.; Du, Y.; Qin, L.; Zhao, X. Morphology and Effect of Load on Bridge Piers Impacted by Continuous Sea Ice. *J. Mar. Sci. Eng.* **2024**, *12*, 1871. https://doi.org/10.3390/jmse12101871

Academic Editor: Mike Meylan

Received: 27 September 2024
Revised: 15 October 2024
Accepted: 15 October 2024
Published: 18 October 2024

1. Introduction

In the project example, cross-sea bridge piers in the winter ice flow period are often hit by the sea ice swarm. The collision of the coupling force generated by the piers and collision avoidance facilities will cause varying degrees of damage and, in extreme cases, even cause the collapse of the bridge piers, the main beams falling off, and other phenomena, and the piers play a role in supporting the superstructure of the bridge. Once the failure occurs, it will cause the instability of the superstructure, which will seriously affect the normal navigation and transport on the sea surface and even bring great losses to people's lives and properties. Therefore, there is an urgent need to carry out the study of the loading pattern and effect of sea ice collision bridge piers in order to explore the impact of bridge piers in the collision effect of the law.

Due to differences in the strength, speed of movement, thickness, shape, and width of the structures, sea ice causes extrusion, creep, buckling, and splitting damage on the surface of upright structures. The different ways of sea-ice damage lead to differences in the forces exerted on the structures. Song et al. [1] regarded sea ice as a semi-infinite structure on an elastic foundation, regarded the buckling damage of the sea ice on the upright structure as a flat plate instability problem under the concentrated force, and gave the critical load of the sea ice under the action of piles and columns. The scaling experiments and field observations are the main parts of the simultaneous loading study, which can provide verification criteria for numerical simulations. Qu et al. [2] analyzed the creep compression force of low velocity sea ice with upright structure by means of experiment and field

monitoring, and concluded that creep compression produces a small force relative to rapid compression damage. Lemström et al. [3] carried out modeling experiments on the process of interaction between ice and inclined structure in shallow water.

With the development of finite element software, numerical simulation has been favored by scholars from all walks of life. Metrikin et al. [4] verified that the errors between experimental and numerical results of the slewing and drag characteristics of a ship model–sea-ice area model in an ice pool were within acceptable limits; Gong et al. [5] simulated the dynamic response of an ice raft and a bridge abutment in an aqueous medium under different collision impact parameters; Zhu et al. [6] used an ice material-based model of sliding loads to investigate the joint action of ice indentation and sliding loads, ice fragmentation, and structural damage results under ice motion trajectory. An ice material model based on a concrete material model was used to simulate the mechanical impact of ice in the ANSYS/LS-DYNA program; Zhang et al. [7] simulated the collision process between flowing ice and a T-rigid bridge pier using LS-DYNA; and Wu et al. [8] proposed a complete bridge analysis model to study the dynamic response of the Bohai Sea-crossing bridge under the random ice loading of floating sea ice. Some scholars have also carried out a large number of studies in combination with the effects of sea traffic on sea ice loading, among which Xia et al. [9] considered the effects of drift ice and established a dynamic analysis model of drift ice loading on the coupled system of the shuttered bridges; Li et al. [10] investigated the excitation effect of the Kaoyong ice on the train. Wang et al. [11] led a team to use numerical simulation to study the dynamic analysis model of a bridge when the ice loading was applied as a static load applied at different locations of hull deformation and collision force, and the structural damage of the hull structure after interaction with ice. However, due to the complexity of ice morphology, most scholars have simplified the ice structure. In order to be closer to the real situation of sea ice morphology, a few scholars have simplified the ice morphology. Kawano et al. [12] found that Voronoi diagrams can be used to construct the geometry of ice crystals; Liu et al. [13] found that the geometry of ice crystals can be constructed by using Voronoi diagrams; Guo et al. [14] analyzed the collision damage of different sizes of drift ice on bridge abutments at different water depths. At present, the research of scholars at home and abroad is mostly experimental studies of different ice morphology and ice impact simulation in the form of ice loading, and the research on the impact of sea ice on sea-crossing bridges is mostly focused on the simulation of large ice and single small ice, while the research on the collision of bridge piers by considering the continuous sea ice in the aqueous medium is relatively little.

At present, scholars at home and abroad mainly focus on the simulation experimental studies for different ice morphologies, especially in the study of ice impact in the form of ice load applied to hydraulic buildings, and most of these studies focus on the simulation of the impact of a large ice cube or a single small ice cube. However, there is still an obvious gap in the research on continuous sea ice impacts on bridge piers in aqueous media, especially on factors such as continuous sea ice spacing, continuous ice mass, and continuous ice area. In order to fill this research gap, we used MATLAB (MATLAB-R2022A) and ANSYS/LS-DYNA (ANSYS-2022-R1/LS-DYNA-LSPREPOST4.3_X64) software to carry out detailed numerical simulations of the collision process between sea ice and bridge abutments based on a specific model of a sea ice area impacting a railway bridge abutment. This study not only contributes to an in-depth understanding of the loading pattern and effect of continuous sea ice on bridge piers, but also provides an important theoretical basis and technical reference for domestic and international cross-sea bridge abutment concrete in coping with the problem of sea-ice collision in order to enhance its safety and durability in extreme marine environments.

2. Continuous Sea-Ice Bridge Pier Impact Finite Element Mode

2.1. Fluid-Solid Coupling

Using the Lagrangian–Eulerian method, the sea ice and bridge abutments are defined as Lagrangian entities, the water and air media are defined as Eulerian entities, and

the coupling of fluid and sea ice structures is achieved through the CONSTRAINED_LAGRANGE_IN_SOLID keyword in LS-DYNA (LS-DYNA-LSPREPOST4.3_X64) software to study the water–air coupling process in the ice collision area of the Yellow River mega-railway bridge of Yinchuan Airport in the course of change rule. The fluid–solid coupling model is shown in Figure 1, in which the water and air domains only cover the sea ice part to simplify the model for calculation.

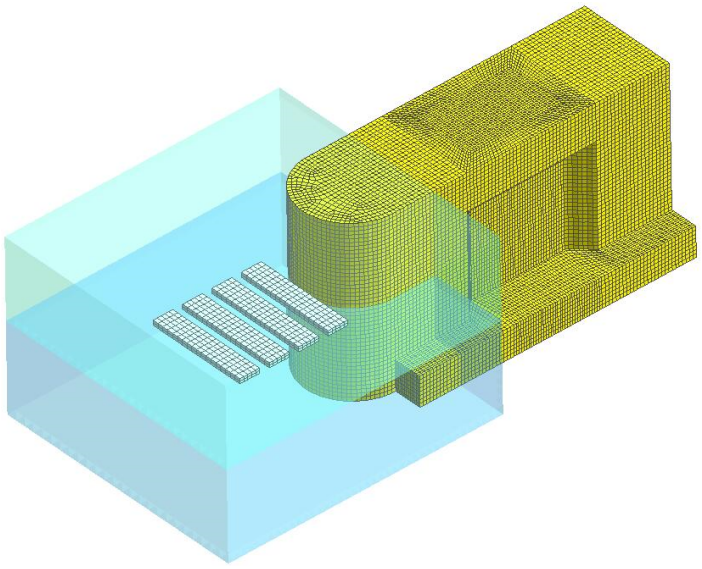

Figure 1. Fluid-structure coupling mode.

2.2. Mesh Convergence Study

In order to study the influence of sea ice and abutment grid size on the numerical simulation results, two groups of ice grids, A_1 and A_2, and two groups of abutment grids, B_1 and B_2, were selected, and the X forward displacements obtained by numerical simulation under different grid sizes are shown in Table 1.

Table 1. Comparison of Peak equivalent stress and X-direction displacement peak at different mesh scales.

Mesh Serial Number	A_1	A_2	B_1	B_2	Experimental Value
Mesh size	$0.05 \times 0.05 \times 0.05$ m^3	$0.07 \times 0.07 \times 0.07$ m^3	$0.05 \times 0.05 \times 0.05$ m^3	$0.08 \times 0.08 \times 0.08$ m^3	
Peak equivalent stress ($\times 10^7$ Pa)	2.617 (4.0%)	2.928 (−7.5%)	2.517 (7.6%)	2.741 (−0.6%)	2.725
X-direction displacement peak ($\times 10^{-4}$ m)	9.749 (0.2%)	10.245 (−4.9%)	9.349 (4.3%)	9.812 (−0.5%)	9.766

From Table 1, the peak equivalent force of the ice grid with the experimental value error of 4.0% and −7.5%, respectively, the bridge abutment grid peak equivalent force with the experimental value error of 7.6% and −0.6%, respectively; the peak x–direction displacement of the ice grid with the experimental value error of 0.2% and −4.9%, respectively, the bridge abutment grid x–direction peak displacement with the experimental value error of 4.3% and −0.5%, respectively. In summary, the ice grid of A_1 ($0.05 \times 0.05 \times 0.05$ m^3) and the abutment grid of B_2 ($0.08 \times 0.08 \times 0.08$ m^3) are used in this paper for numerical calculation.

2.3. Selection of Model Material Parameters

The concrete continuous surface cap model CSCM developed by the Federal Highway Administration is used to simulate the dynamic performance and damage characteristics

of bridge piers under the impact, and the keyword *MAT_CSCM_ CONCRETE is added to define it. Ice material parameters refer to the research results of Yang [15] and other research results; the 13th material *MAT_ISOTROPC_ELASTIC _FAILURE in the LS-DYNA material library is selected to simulate the characteristics of ice, and the model parameters are set as in Tables 2 and 3.

Table 2. Parameters of concrete material model.

LS-DYNA Model Parameter	Numerical Value	Unit
RO (mass density)	2500	/(kg·m^{-3})
RECOV (coefficient of recovery)	10	
FPC (free compressive strength without lateral limit)	29	MPa
DAGG (maximum aggregate size)	0.02	m

Table 3. Ice material parameters.

LS-DYNA Model Parameter	Numerical Value	Unit
RO (material density)	910	/(kg·m^{-3})
G (shear modulus)	2.2	GPa
SIGY (yield stress)	2.136	MPa
ETAN (plastic modulus)	4.26	GPa
BULK (bulk modulus)	5.26	GPa
EPF (Plastic strain at failure)	0.35	–
PRF (truncation stress)	−3.0	MPa

Referring to the setup of Gong [16] and others, the water and air media are described by means of an intrinsic model and an equation of state, using *MAT_NULL material to describe the water and air media, and the equations of state are realized by means of EOS-GRUNEISEN and EOS-LINER-POLYNOMIAL,

The Gruneisen equation of state is as follows:

$$P = \frac{\rho_0 C^2 \mu \left[1 + \left(1 - \frac{\gamma_0}{2}\right)\mu - \frac{\alpha}{2}\mu^2\right]}{\left[1 - (S_1 - 1)\mu - S_2 \frac{\mu^2}{\mu+1} - S_3 \frac{\mu^3}{(\mu+1)^2}\right]^2} + (\gamma_0 + \alpha\mu)E \quad (1)$$

where P is the pressure; $\mu = \rho/\rho_0 - 1$; $C, S_1, S_2, S_3,\ \gamma_0$ are the equation coefficients.

The linear polynomial equation of state is as follows:

$$P = C_0 + C_1\mu + C_2\mu^2 + C_3\mu^3 + \left(C_4 + C_5\mu + C_6\mu^2\right) \quad (2)$$

where P is the pressure, $\mu = \rho/\rho_0 - 1$; $C_0,\ C_1,\ C_2,\ C_3,\ C_4,\ C_5,\ C_6$ are polyno-mial equat-ion coefficients.

Parameters are set as in Table 4.

Table 4. Water medium state equation parameters.

LS-DYNA Model Parameter	Water Medium	Air Medium	Unit
Density RO	998	1.29	/(kg·m^{-3})
Cut-off pressure PC	-10×10^5	−10	Pa
Constant C	1647	0	
Constant S_1	1.92	0	
Constant S_2	−0.096	0	
Constant γ_0	0.35	0	
Coefficient C_4	0	0.4	

2.4. Ice-Abutment Impact Finite Element Modeling

2.4.1. Bridge Pier Model

As shown in Figure 2, a bridge pier in a sea-crossing bridge is selected, which is taken as 5.63 m in length, 1.95 m in width, 3.42 m in height, and 3.07 m in width at the bottom of the pier, with a circular collision avoidance body at the front and a diagonal inward 45° excavation depth of 0.36 m in the middle of the pier. The bridge pier was meshed finely by Hypermash software (Hypermash2022), imported into LS-DYNA modeling, and constrained by using the constraint keyword SET_NODE_LIST_(TITLE) in LS-DYNA to constrain all degrees of freedom of the base plate of the pier in all three directions, and the other surfaces were free surfaces. In the process of the impact of the sea ice layer on the bridge abutment, there will be an ice body damage erosion phenomenon. In order to ensure that in the ice body broken unit failure deletion, the ice and the bridge remain in contact with each other after the computation, the use of LS-DYNA in the contact keyword CONTACT_ERODING_ SURFACE_TO_SURFACE defines the erosion of the contact, the sea ice body for the slave surface (SSID), and the bridge abutment for the master surface (MSID). The sea ice body is the slave surface (SSID), the bridge abutment is the master surface (MSID), and the coefficient of static friction (FS) and the coefficient of kinetic friction (FD) are taken as the values of 0.15. In the finite element numerical simulation, the sea ice, bridge abutment, water medium, and air medium are all used in the single-point integration. Solid164 solid cells avoid the volume locking of the cells.

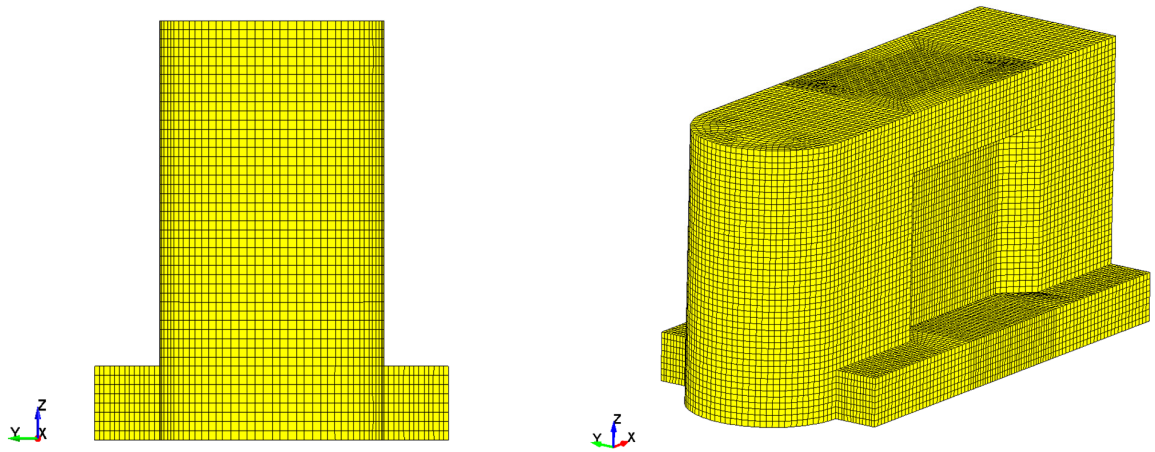

(**a**) (**b**)

Figure 2. Mesh division of bridge pier: (**a**) main view (**b**) overall view.

2.4.2. Icebreaker Model

By statistically analyzing the existing data on sea ice bodies, a realistic distribution model of sea ice bodies is constructed based on the parameters of the size, shape, and density of the sea ice bodies. In this model, the main study is the influence factor of continuous sea ice collision, i.e., limiting the collision area of sea ice based on the actual observation of sea ice and previous research experience to select a sea ice body of 2 m × 0.4 m with a thickness of 0.1 m. Between ice and ice in the process of sea ice collision, an abutment will appear in the front row of ice in the impact of the abutment after the rebound and the rear row of ice collision, ice, and ice collision after the extrusion of the ice body crushing, to ensure that the sea ice continues to continue to collide with the bridge abutment, ice, and ice collision with the LS-DYNA in the one-sided contact. The keyword CONTACT_ ERODING_SINGLE _SURFACE defines the ice eroding contact with ice. The horizontal direction only considers the dragging force of the water flow on the sea ice; the initial velocity of the ice is chosen as the x–direction to provide power for the ice; the spacing between the sea ice body and the collision force between the shape of the sea ice and the abutment are considered; you can simulate the process of interaction between the sea ice

and the abutment, and assess the degree of impact of the sea ice on the abutment, according to the real-time data measured by Hu [17], which are equal to the ice period from 2011 to 2020; the velocity of 1 m/s of the sea ice area is selected. Using discrete element analysis, the stability and safety of the bridge structure can be investigated under different ice-breaking conditions. By analyzing the movement trajectory of the sea ice body, the magnitude of the collision force, and other parameters, it is possible to assess the stress condition of the bridge piers and the potential risk of damage.

- Ice break-up spacing

Under the hydrodynamic air coupling mechanism, the collision of sea ice with the bridge abutment is not only the traditional collision problem between the abutment and ice, but also the collision problem between sea ice and overall ice. Therefore, not only must the impact of the speed of sea ice be considered, but the influence of the ship on the collision problem of the sea ice layer, sea ice spacing, and other parameter interactions must also be drawn on. In order to facilitate the calculation, the size of the calculation waters and air domain is reduced, the horizontal direction of the bridge ice collision spacing is shortened, and only the destructive effect of the impact force on the bridge abutment in a short time in the transverse direction and the subsequent impact of extrusion in a short time are considered. The high-speed frontal collision and extrusion are analyzed by finite element analysis. Considering the impact of continuous collision on the bridge abutment, i.e., the impact effect of sea ice with different spacing on the bridge abutment, according to the research of Wang [18] et al. (real-time data obtained through the UAV platform on 25 April 2021), the distribution density of the ice is 81.05% maximum, and the minimum is below 10%. A simple calculation yielded a spacing of sea ice between 0.15 m and 0.66 m. Therefore, four ice spacings of 0.2 m, 0.4 m, 0.6 m, and 0.8 m were selected for collision simulation, where 0.8 m is the value taken into account for extreme cases.

- Mass of sea ice cubes

Referring to the study of Yu [19] and others, the diameter of sea ice in the ice area usually ranges from 0.5 m to 8 m, and the corresponding area ranges from 0.8 m^2 to 200 m^2. The upper reaches of the Yellow River are mainly dominated by sea ice during the opening period, so sea ice areas with averages of 0.8 m^2, 1.2 m^2, 1.6 m^2, and 2 m^2 were selected for the study. By observing the flow ice in the section of Yinchuan Airport Yellow River Special Bridge, considering the ice condition of the Yellow River, the geographic location of Yinchuan Airport Special Bridge, and referring to the research of Chen [20] and others' research on flow ice, the thicknesses of 0.05 m, 0.1 m, 0.15 m, and 0.2 m of sea ice were selected for the study.

- Different shapes of sea ice

Combining different sea ice spacing conditions and different sea ice average area conditions, referring to the research of Zhu et al. [21], the two-dimensional Voronoi diagrams are generated by applying the MATLAB programming software referencing the exclusion method and the perturbation method, and the different shapes of the sea ice impact piers are investigated. The Voronoi diagrams are also referred to as the Dirichlet diagrams or the Tyson polygons, and the Voronoi diagram method is a geometric segmentation method that forms polygon boundaries by dividing the plane into a series of regions, where each region contains all points nearest to a point within that region. In the 2D Voronoi diagram of broken ice, each broken ice piece is considered a point, and the region around each broken ice piece is the corresponding Voronoi region of that broken ice piece. Considering these points as seeds, the exclusion and perturbation methods are introduced to control the degree of regularity, i.e., uniformity, of the distribution of the seed points.

Firstly, the number of seed points n and the ice area A are predetermined by introducing the geometric regularity parameter *delta* (with values ranging from 0 to 1) = d/d_{max}, and the maximum distance dmax for the repulsion method is calculated.

$$d_{max} = \sqrt{2A/\sqrt{3}n} \tag{3}$$

Then, the uniformly distributed initial seed points are generated, and the repulsion method is used to generate the Voronoi seed points. Finally, the perturbation method is used to adjust the position of the seed points, where the radius of the perturbation circle r is:

$$r = 0.1 \times d_{max} \tag{4}$$

The perturbation amount delatp is:

$$delta_p = (1 - delta) \times d_{max}/10 \tag{5}$$

The generation of two-dimensional fragmented ice areas with different geometrical regularities is shown in Figure 3.

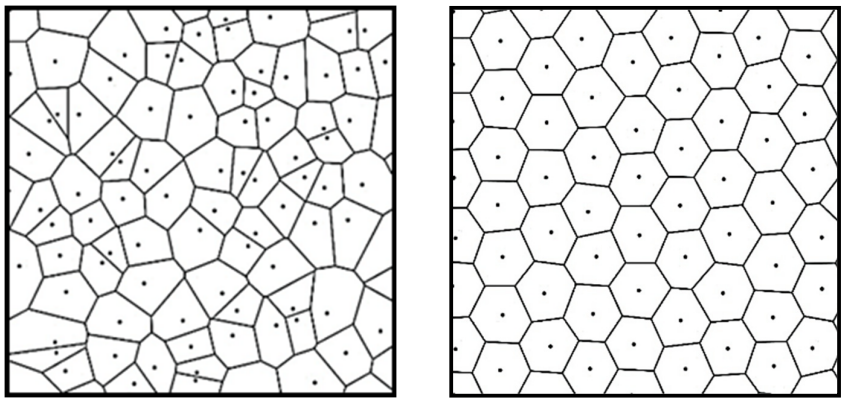

(**a**) (**b**)

Figure 3. Two-dimensional Voronoi diagrams with different degrees of regularity: (**a**) *delta* = 0.1; (**b**) *delta* = 1.0.

In the case of selecting the same 2D (*delta* = 0.1) Voronoi diagram, different sizes of sea-ice area can be chosen by intercepting sea ice at different locations to achieve diversified effects. The specific steps are as follows:

1. Segment the Voronoi diagram: use the Voronoi segmentation algorithm to divide the 2D space into multiple non-overlapping regions, each representing the location of one sea ice cube.
2. Cutting regions: select regions at different positions and intercept them as needed. The location of the intercept can be determined by random selection, specifying the co-ordinate range of the region, or other methods.
3. Adjusting the size of crushed ice: For each intercepted region, adjust the size of the crushed ice as needed. Adjustments can be made based on the size of each region, a scale factor, or using a different scaling algorithm. Larger regions can generate larger crushed ice cubes, while smaller regions can generate smaller crushed ice cubes.
4. Generate shattered ice cubes: Based on the adjusted shattered ice cube size, randomly generate shattered ice cubes of corresponding size and shape in each intercepted region. A randomized algorithm can be used to generate the shapes of the sea ice cubes to ensure that there is a diversity of sea ice cubes within each region.

In this way, it is possible to select different locations of sea ice cubes on the same Voronoi diagram and size them according to the intercepted area to achieve the effect of

different sea ice area sizes. This can increase the diversity and realism of the sea ice and fit the actual situation to study the overall effect of different spacing of different average areas on the bridge pier. As shown in Figure 4, sea ice with average areas of 1 m^2, 1.5 m^2, 2 m^2, and 2.5 m^2 were selected, respectively.

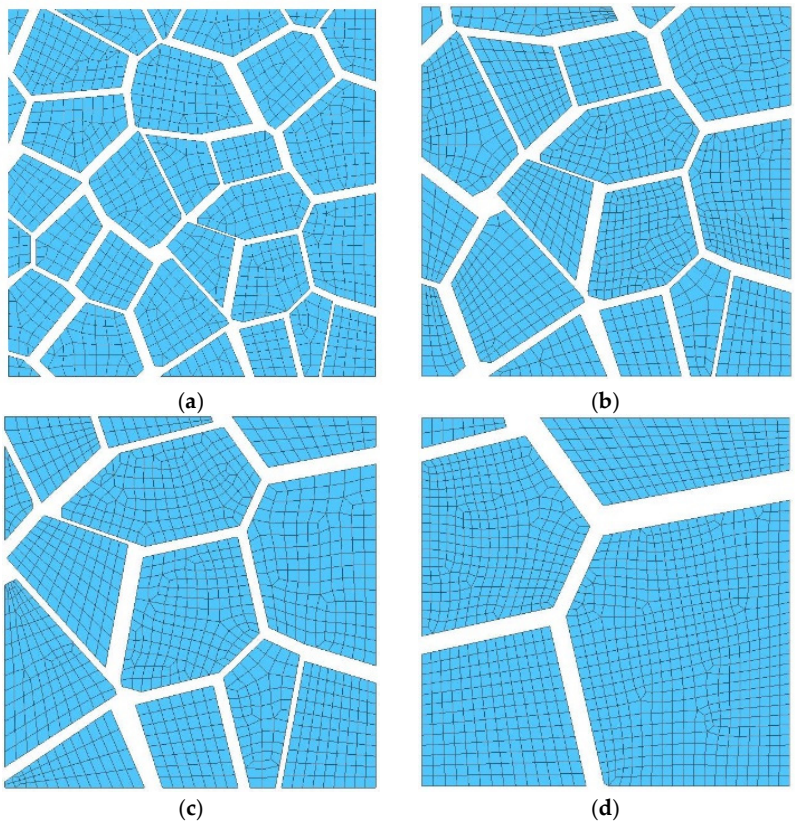

Figure 4. Average area of different sea ice blocks sea ice area: (**a**) A_0 = 1.0 m^2; (**b**) A_0 = 1.5 m^2; (**c**) A_0 = 2.0 m^2; (**d**) A_0 = 2.5 m^2.

3. Analysis of Parameters Affecting Ice-Pier Collision

3.1. The Impact of Different Spacing of Sea Ice on the Bridge Pier

Simulation results found that, along with the water cushion effect, the bridge pier by the impact area is mainly affected by the continuous collision of sea ice and the continuous extrusion effect. The continuous sea-ice collision railway bridge abutment is mainly divided into three stages: the first collision stage, the continuous collision stage, and the extrusion stage. Each stage is analyzed and illustrated by the equivalent stress diagram, and the impact force is calculated and derived by the keyword DATABASE_ASCLL_option. Four horizontally arranged sea-ice bodies of 0.1 m thickness, 2 m length, 0.4 m width, and 1 m/s speed were selected to collide with the bridge abutment, and the calculation time was increased with the spacing.

As shown in Figure 5, the sea-ice spacing of 0.2 m, the first row of sea ice collision with the bridge abutment rebound, and the rear row of ice collision rebound again, result in a continuous chain collision, i.e., the continuous collision stage (0.01 s~0.75 s), the sea ice spacing is small, the subsequent ice collision acceleration time is shorter, and continuous collision leads to the failure of the sea ice broken at the same time, accompanied by the emergence of the phenomenon of stress concentration; the stress is centered in the location of the collision contact. Subsequently, the chain collision of rows of ice is transmitted and diffused step by step, and finally concentrated in the ice–ice contact surface area. Subsequently, the extrusion phase (0.75 s~1 s) of the equivalent force of the bridge pier increases step by step with time, and it can be seen from the equivalent force cloud diagram that the extrusion stress is much larger than the impact stress. As shown in Figure 6, the

sea-ice spacing is 0.4 m, the spacing is the same as the width of the sea ice, in the continuous collision stage (0.01 s~1.18 s) the number of multiple collisions is reduced, the second row of sea ice appeared along the y–direction climbing phenomenon, the sea ice did not appear obviously broken, the stress concentration phenomenon is mainly concentrated in the ice impact location, in extrusion stage (1.18 s~1.5 s) the piers equivalent effect force rising speed has slowed down, the sea ice climbing phenomenon is more obvious, and the covering phenomenon occurs between the ice blocks with the passage of time. As shown in Figure 7, the sea ice spacing 0.6 m, in the continuous collision stage (0.01 s~1.7 s) the sea ice climbing phenomenon increased significantly, and part of the ice overturned because the spacing of 0.6 m in the sea ice transverse size of 0.4 m gap is small and there is enough distance to make the sea ice overturn; the latter two rows of ice collide with the first two rows of ice when the speed did not slow down, and the first row of ice accelerated in the successive collision after a significant increase in the extrusion stage (1.7 s~2 s). With the sea ice climbing superimposed on the overall offset, lateral squeezing pressure increased significantly, and the effect of sea ice spacing at different angles can be considered subsequently. As shown in Figure 8, the sea ice spacing is 0.8 m, the continuous collision stage (0.01 s~2.4 s) due to the spacing in the sea ice lateral size is larger, the sea ice occurs after the flip, and the subsequent sea ice is covered together; the chain collision phenomenon is not obvious and the impact time span is larger. With the passage of time, the probability of extrusion overlap occurring in the extrusion stage (2.4 s~2.5 s) is significantly increased compared with other conditions.

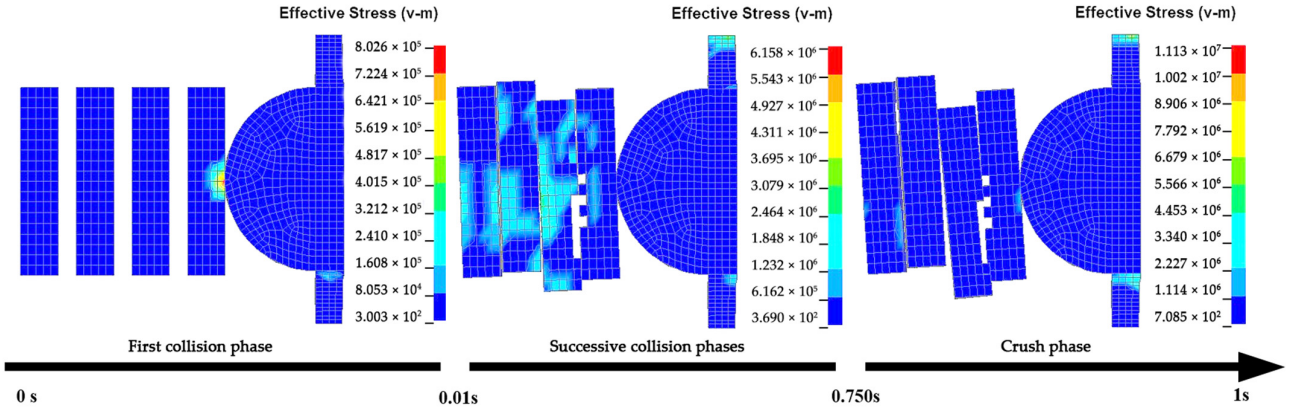

Figure 5. The maximum impact force of 0.2 m between sea ice corresponds to the equivalent stress cloud map.

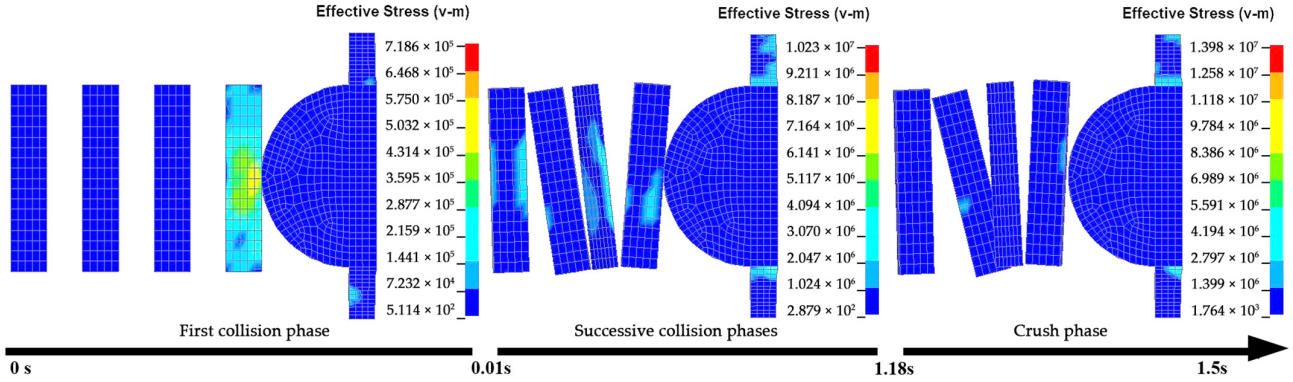

Figure 6. The maximum impact force of 0.4 m between sea ice corresponds to the equivalent stress cloud map.

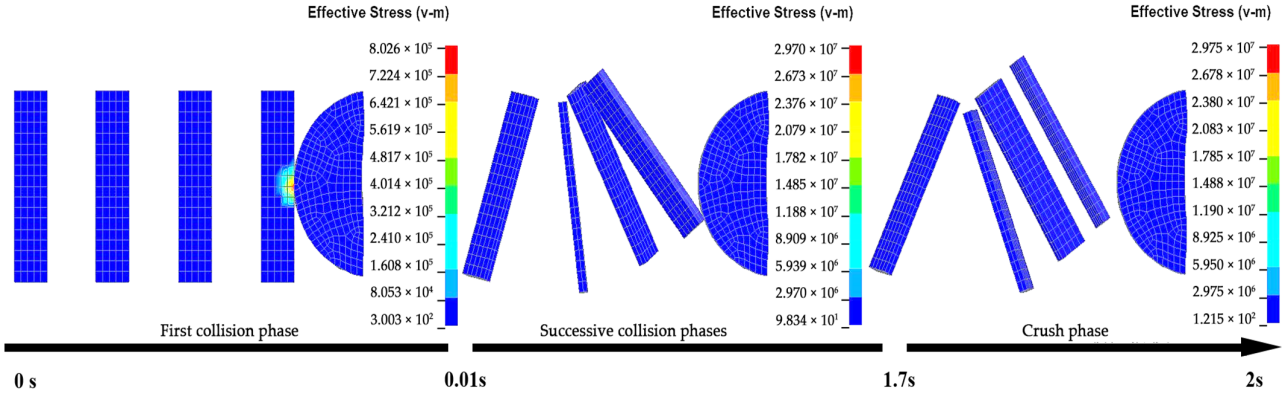

Figure 7. The maximum impact force of 0.6 m between sea ice corresponds to the equivalent stress cloud map.

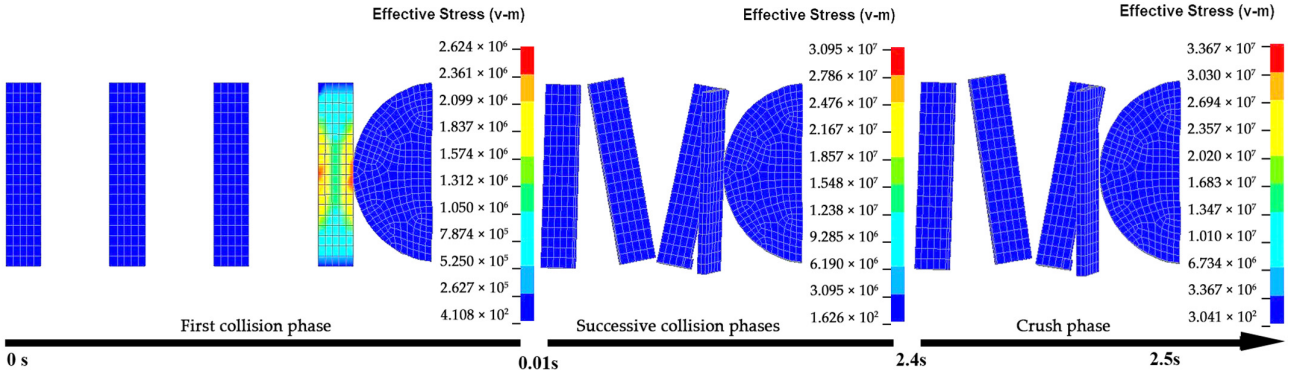

Figure 8. The maximum impact force of 0.8 m between sea ice corresponds to the equivalent stress cloud map.

Figure 9a shows the peak impact force, and sea-ice spacing of 0.2 m continuous collision more often; sea-ice spacing of 0.4 m secondary impact force peak obviously increased compared to the spacing of 0.2 m conditions; sea-ice spacing of 0.6 m in two rows of ice climbing impact the first row of ice, acceleration increased significantly, and the peak of the second collision is higher than the peak of the first collision; sea-ice spacing was 0.8 m after the row of ice speed decreased significantly on the second collision pier; the second impact on the bridge abutment is obviously reduced. Figure 9b is the equivalent force curve of the bridge abutment at the location of the collision, the sea ice's continuous impact on the bridge abutment when the equivalent force is obviously a peak phenomenon, the extrusion stage of the equivalent force slowly upward into the incremental trend, and with the passage of time the extrusion stress will be more than the impact stress to reach the maximum value, such as in Figure 9b 0.8 m spacing conditions. In summary, under different spacing, the ice sheet collided with the bridge abutment to form a continuous chain collision; the spacing gradually increased, resulting in a decrease in the collision force; the abutment equivalent force gradually increased, and with the passage of time the extrusion stage equivalent force is greater than the collision stage equivalent force. To sum up, the sea-ice continuous collision stage spacing was 0.6 m on the pier impact force maximum 60 kN, the impact is obvious, the extrusion stage of different spacing conditions of sea ice are extrusion obvious, and the stability of the bridge pier has a greater impact.

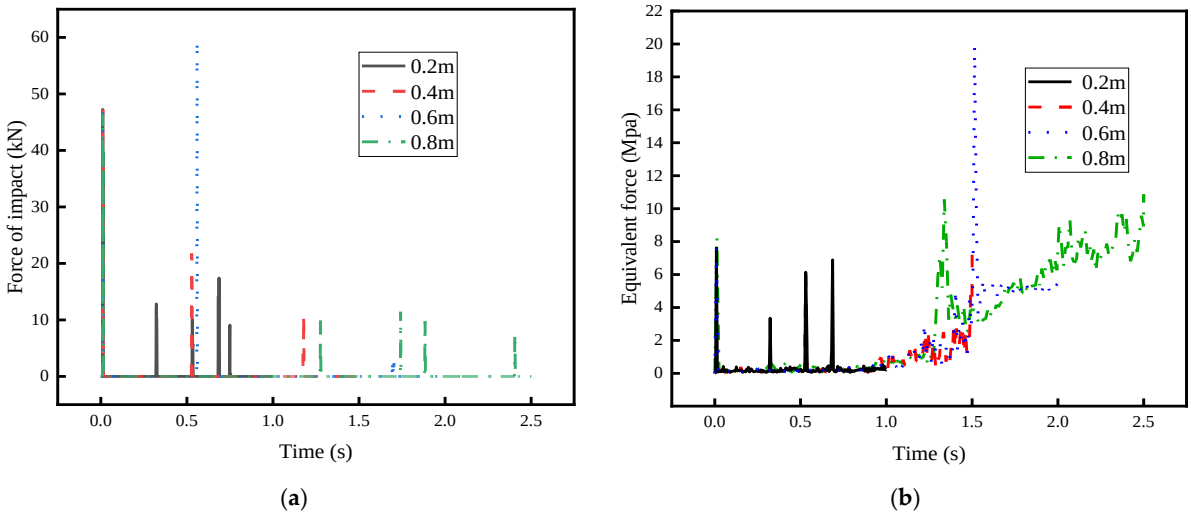

(**a**) (**b**)

Figure 9. (**a**) Peak ice load diagram; (**b**) equivalent stress diagram.

3.2. Effect of Different Crushed Ice Masses on Bridge Abutments

Four horizontally arranged sea ice bodies of 2 m in length and 1 m/s velocity are selected to collide with the bridge pier. The sea ice thickness of 0.1 m was determined and the sea ice area changed by changing the sea ice width; the sea ice width of 0.4 m was changed by changing the sea-ice thickness of the integrated mass working conditions.

3.2.1. Area of Different Sea Ice Masses

Only the effect of the average area of different sea ice on the bridge abutment under the influence of different shapes was considered. As shown in Figure 10, the average area of different sea-ice rows was in collision with the abutment with the back row of ice and produced a continuous chain collision; sea ice began to break, accompanied by the emergence of stress concentration phenomenon, and the stress diffusion phenomenon with the increase in the average area tends to flatten out, while the maximum impact force occurs in the initial stage of collision in the subsequent stage of the extrusion collision. The abutment equivalent force is mainly distributed in the sea ice and abutments in contact with the side of the neighboring regions, namely the lower abutment connection. As the average area increases, the mass increases, the number of consecutive positive collisions decreases, the squeeze phase is advanced, and the equivalent force climb does not see an obvious pattern. As shown in Figure 11, the larger the average area, the greater the impact of continuous collision. The maximum impact force peak and the second largest impact force peak are linearly increasing, that is, under the same premise of the spacing, the acceleration of continuous collisions of sea ice will decrease step by step. The second largest impact force is manifested in the larger quality of the impact force, which shows that the effect of the mass of the sea ice impact on the bridge abutment is much larger than the impact of acceleration on the sea ice impact on the bridge abutment. The second largest impact force shows that the larger the mass, the larger the impact force. In summary, with the change of the shape of the sea ice, i.e., the average area of the sea ice increases, and the impact force on the bridge abutment increases step by step.

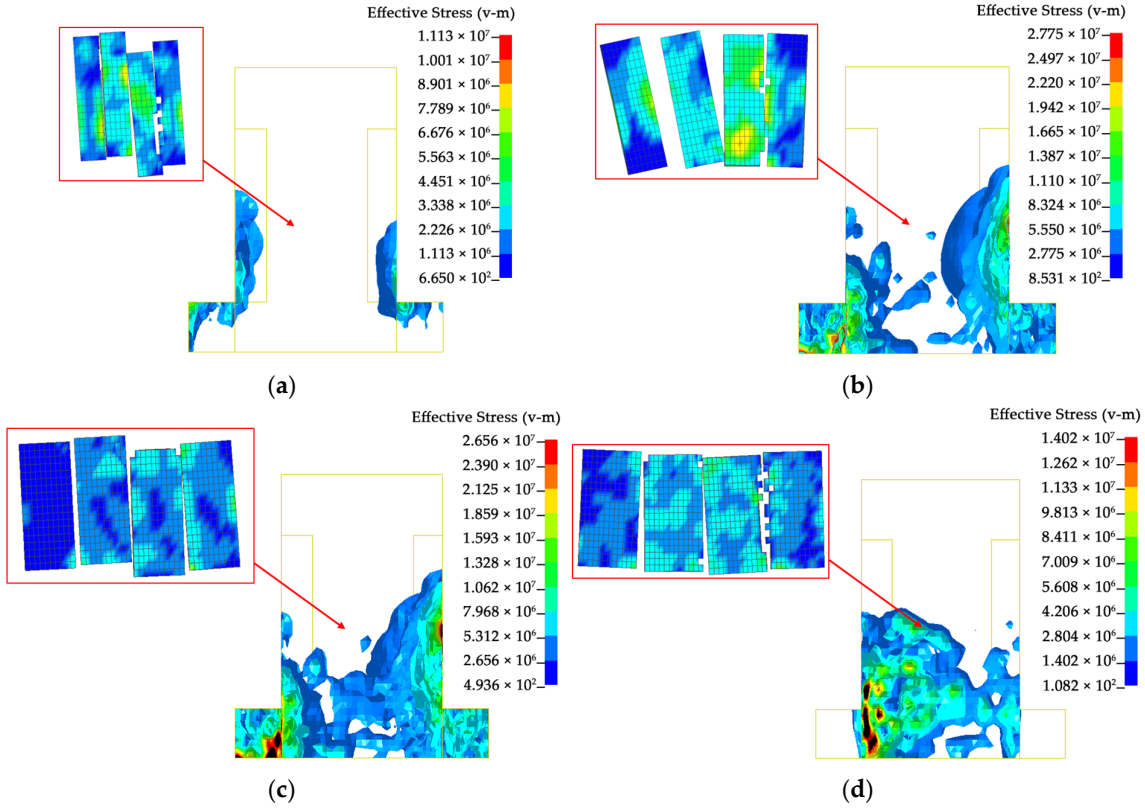

Figure 10. Maximum equivalent stress cloud map of different ice mass area: (**a**) A_0 = 0.8 m^2; (**b**) A_0 = 1.2 m^2; (**c**) A_0 = 1.6 m^2; (**d**) A_0 = 2.0 m^2.

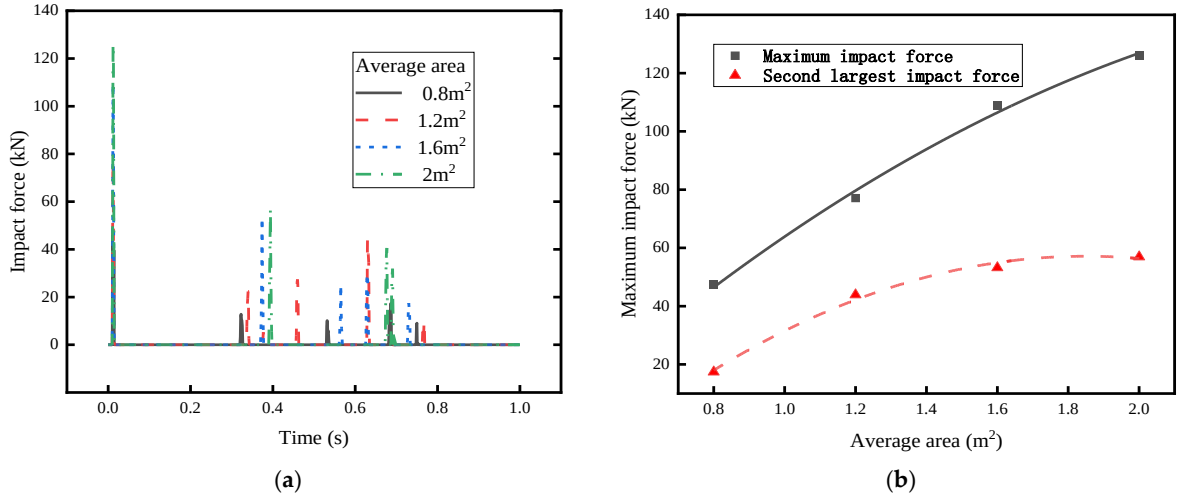

Figure 11. (**a**) Map of peak ice load with different sea ice area; (**b**) impact force curves for different ice cube areas.

3.2.2. Different Thicknesses of Sea Ice

Only the impact of different ice thickness on the bridge abutment under the influence of different shapes is considered. As shown in Figure 12, there are different sea-ice thickness ice rows in the collision with the bridge abutment with the back row of ice to produce a continuous chain collision. Sea ice was not obviously broken there is an abutment by the impact side of the stress concentration phenomenon, the equivalent force with the thickness increases step by step, the maximum impact force occurs in the initial collision stage, with different sea ice area conditions being the same as in the subsequent squeeze collision stage, the abutment equivalent force is mainly distributed in the sea ice, and the abutment

contact is adjacent to the region of the side that is the lower abutment connection. The abutment contact is adjacent to the side of the region, i.e., the lower abutment connection. As the thickness increases, the mass increases, and the sea ice in many collisions occurs after the climb flip phenomenon, such as in Figure 12a which shows the thickness of 0.05 of the front side of the sea ice in the impact of the abutment after the climb. The back row of ice and the front side of the ice did not see the obvious extrusion phenomenon, such as in Figure 12d, which shows the thickness of 0.2 m of the sea ice layer last lateral flip extrusion abutment. With the increase in the thickness of the sea ice, the sea ice layer extrusion abutments became a more pronounced phenomenon. As shown in Figure 13, the greater the thickness, the greater the impact of continuous collision; the maximum impact force peak and the second largest impact force peak are linearly increasing, and the second largest impact force shows that the larger the mass, the larger the impact force. In summary, with the change of the shape of the sea ice, i.e., the thickness of the sea ice increases, the impact force on the bridge pier increases step by step.

The combination of ice mass, i.e., area and thickness, will determine the actual impact effect; with the increase in area and thickness, the impact force is linearly increasing. The large mass of ice with large area and thickness has higher kinetic energy, and the impact force on the abutment is larger, while the small mass of ice with small area and thickness is lower, but the frequent impact of ice may cause long-term fatigue on the abutment, and according to the change of the second largest impact force, we can judge that the impact of quality on the impact of ice on the abutment is much larger than the impact of acceleration on the impact of ice on the abutment. Overall, the impact of different masses of sea ice on bridge abutments will cause some damage to the bridge abutments, especially in the case of large masses, large areas, and thick ice. In order to protect the bridge structure, measures are usually taken to minimize this risk, such as setting up guards around the bridge or carrying out regular inspections and maintenance.

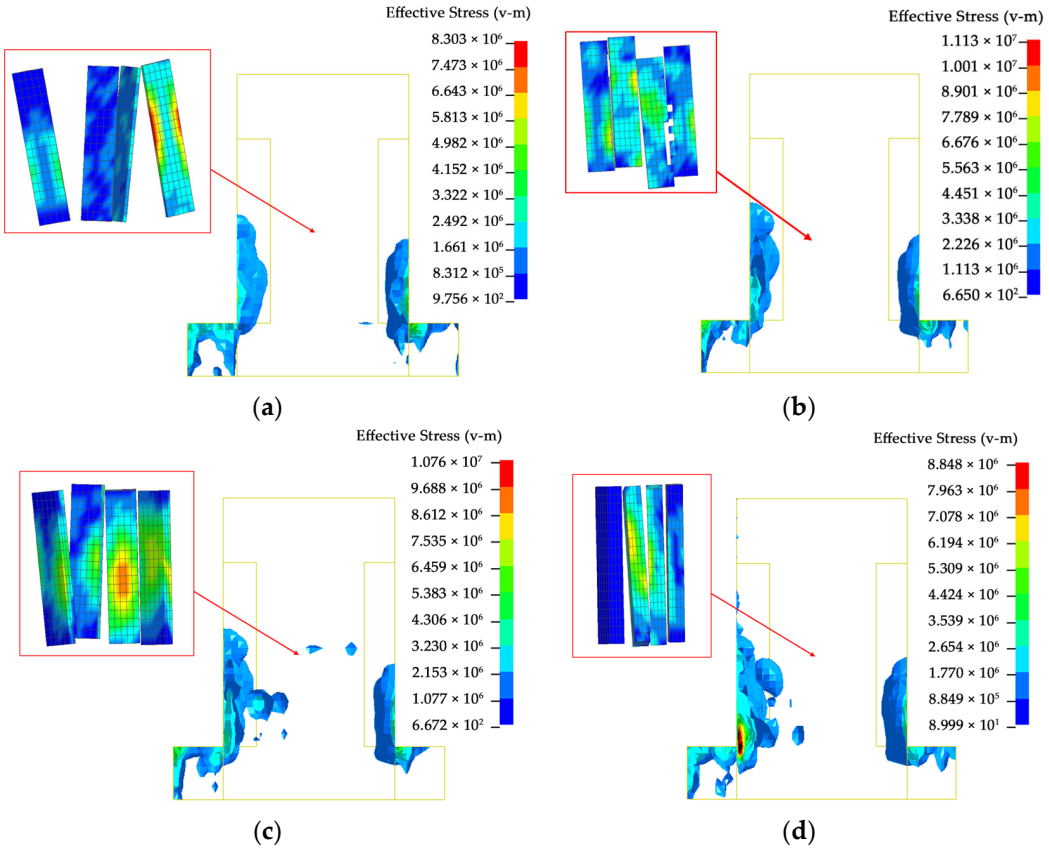

Figure 12. Maximum equivalent stress cloud map for different thickness of sea ice: (**a**) thickness = 0.05 m; (**b**) thickness = 0.1 m; (**c**) thickness = 0.15 m; (**d**) thickness = 0.20 m.

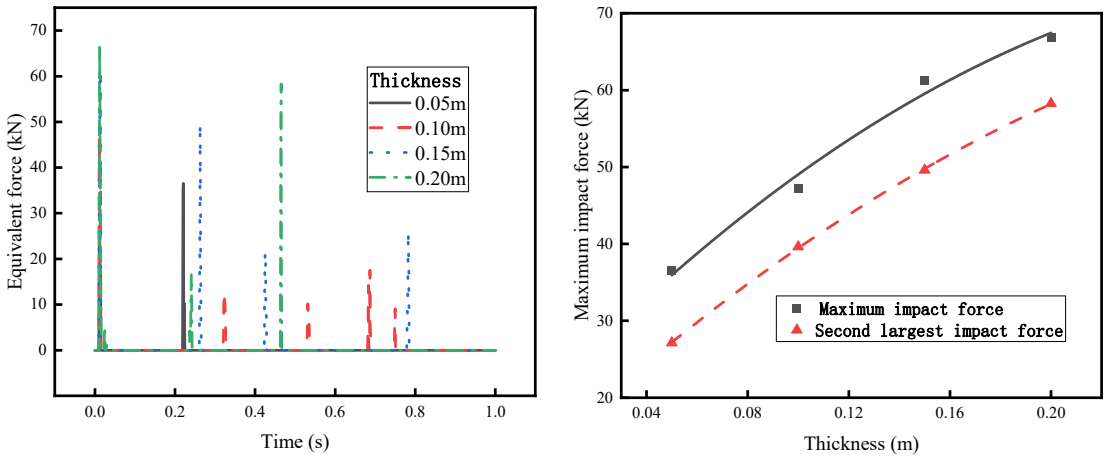

(**a**) (**b**)

Figure 13. (**a**) Peak ice load map with different thickness of sea ice; (**b**) impact force curve of different ice thickness.

3.3. Impact of Different Shapes of Sea Ice on Bridge Abutments

Through the LS-DYNA keyword setting, the mass of sea ice, speed (1 m/s), density, density of sea-ice distribution (80%), and the design and strength of the bridge abutment are set to fixed values, and only the effect of the average area of different sea ice on the bridge abutment under the influence of different shapes is considered.

Figure 14 shows the average area of different sea-ice rows and piers after the collision of the back row of ice to produce a continuous chain collision, and sea-ice collision after breaking, accompanied by the emergence of the phenomenon of stress concentration; the stress diffusion phenomenon with the increase in the average area tends to flatten out, the maximum impact force of larger ice occurs in the first collision stage, followed by the sea ice appearing to be an obvious extension of the *y*–axis climbing phenomenon, and then into the extrusion stage. As shown in Figure 15a, in the process of collision between sea ice and bridge abutment, the equivalent force of bridge abutment is mainly distributed around the adjacent area of contact between sea ice and bridge abutment. And in the location of the collision contact between the sea ice and the abutment, the abutment is impacted by the region of the stress concentration phenomenon. As shown in Figure 15b, the average area of 1 m^2 of sea ice is due to the small average area, the mass of the sea ice, and the impact force are relatively small, and the impact on the abutment is small. It causes some impact and friction on the surface of the bridge abutment without causing serious damage. Shattered ice with an average area greater than 1.5 m^2: this size of shattered ice increases in size step by step, with higher mass and impact forces, and more pronounced impacts on the bridge abutments. Larger ice fragments may cause larger impact forces, resulting in damage to the surface of the bridge abutment. In addition, larger sea ice may also accumulate around the abutments, increasing the impact force of the water flow on the abutments, which can lead to the increased structural instability of the abutments. In summary, as the shape of the sea ice changes, i.e., the average area of the sea ice increases, the maximum impact force on the bridge abutment increases step by step.

It should be noted that the specific impact also depends on the velocity and density of the sea ice; if the velocity of the sea ice is higher or the density is larger, even if the average area is smaller, it may still cause a larger impact force on the bridge pier. Therefore, when assessing the impact of different average areas of sea ice on the bridge pier, it is necessary to comprehensively consider the velocity, density, and other factors.

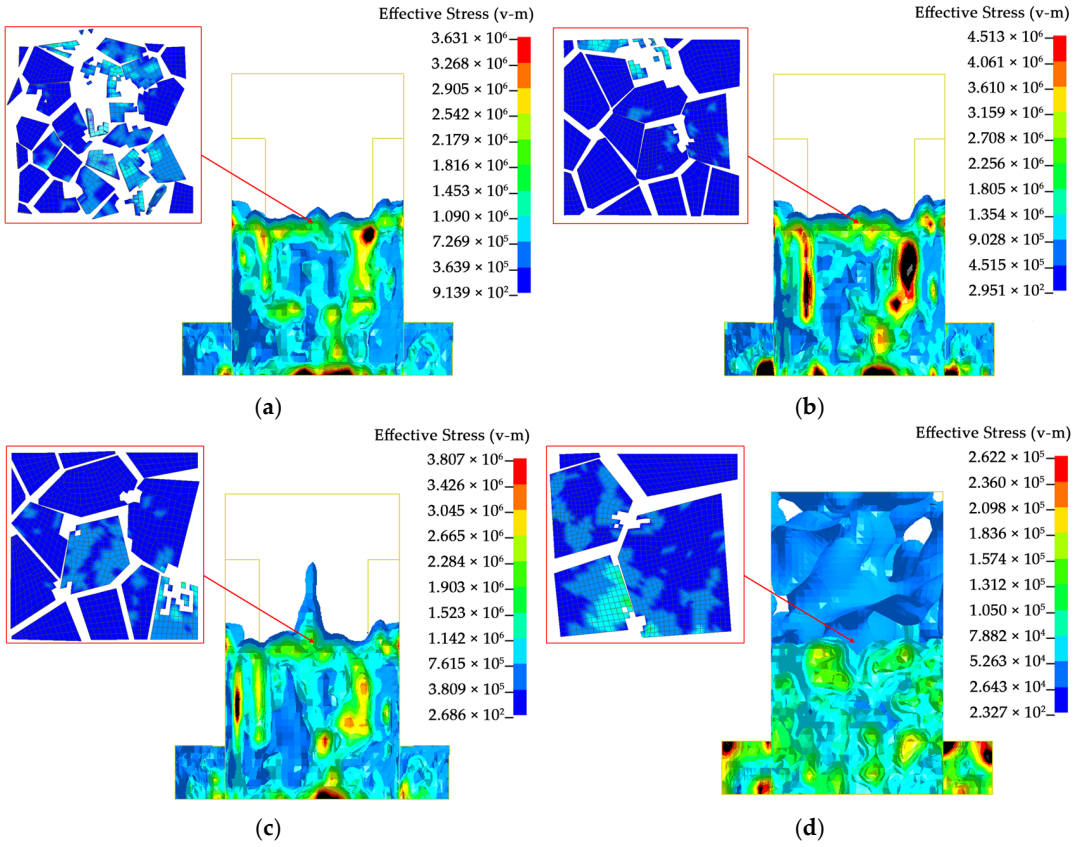

Figure 14. Equivalent stress nephogram of compressive pier with different shapes of crushed ice: (**a**) A_0 = 1.0 m^2; (**b**) A_0 = 1.5 m^2; (**c**) A_0 = 2.0 m^2; (**d**) A_0 = 2.5 m^2.

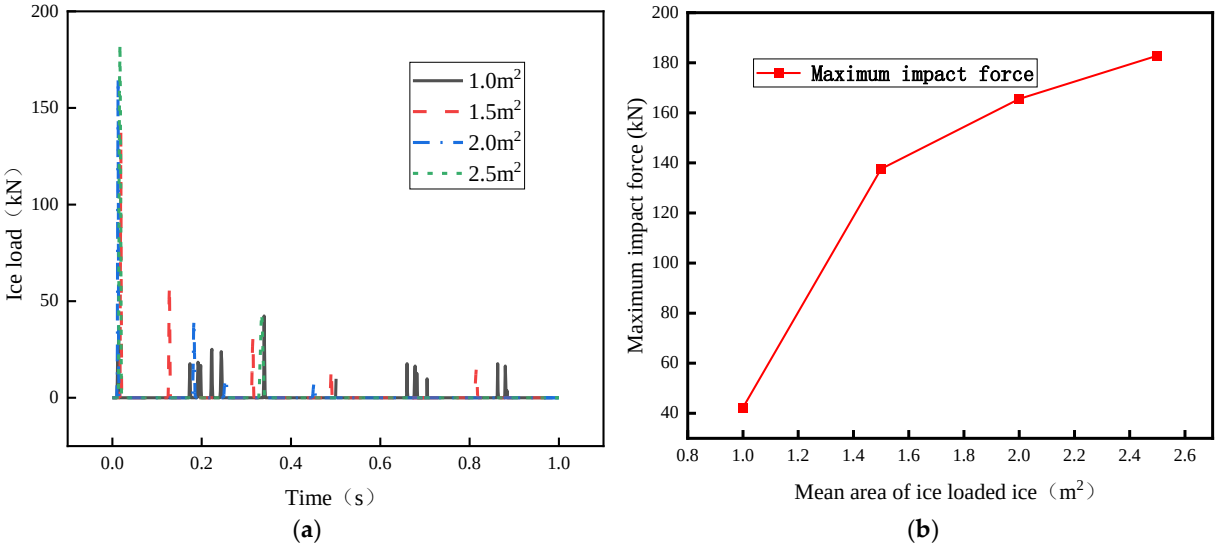

Figure 15. (**a**) Peak ice load of different shapes of sea ice; (**b**) maximum impact force curves of different shapes of sea ice.

4. Maximum Impact Force Verification Experiment

As shown in Figure 16, in order to verify the impact effect of small- and medium-sized drift ice on bridge piers, the experimental steps are as follows:

- Experimental preparation

The use of rectangular water tanks to simulate the water medium and the pier lining selection of C30 concrete slabs installed in the water tank to simulate the real bridge pier force situation.

- Equipment commissioning

Zeroing of all instruments to ensure the accuracy of the measurement of each instrument. Check whether each instrument works properly, including force sensors, speed sensors, and data recording equipment, to ensure the reliability of the data in the experimental process.

- Sea ice body preparation

Fix the crushed ice on the propeller to ensure the stability of the ice body. Adjust the position of the sea ice so that it is precisely aligned with the impact position of the bridge pier.

- Experimental operation

Start the power unit and set the motion parameters of the ice body according to the preset design ice speed and stroke so that the ice body accurately impacts the bridge pier.

- Data acquisition and analysis

Record the maximum impact force peak data of the ice body impacting the bridge pier. The experimental data were compared with the simulation results to analyze the effect of continuous collision of four different areas (0.8 m^2, 1.2 m^2, 1.6 m^2, and 2 m^2) of fragmented ice.

Sixteen groups of four sea ice bodies with widths of 0.4, 0.6, 0.8, and 1.0 m, length of 2 m, spacing of 0.2 m, and speed of 1 m/s were selected for experimental study. Through these steps, the experiment aims to evaluate the impact force of sea ice on bridge abutments at different areas in order to provide data support for actual bridge design and maintenance.

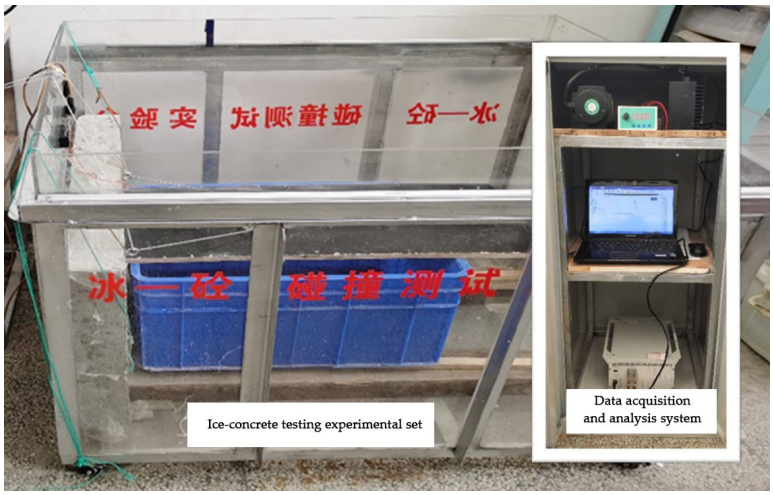

Figure 16. Ice–concrete collision test bench.

Figure 17a shows the magnitude of equivalent force when different average sea ice areas impact the bridge pier. It can be found that the irregularity of the peak equivalent force, the maximum equivalent force in the continuous collision stage, is under the condition of 1.6 m^2 of sea-ice area, and the maximum impact equivalent force does not occur in the first impact, which indicates that the maximum damage to the bridge pier by the sea ice under the effect of the continuous positive collision is brought about by the second impact, and there is no obvious regularity with the sea-ice area.

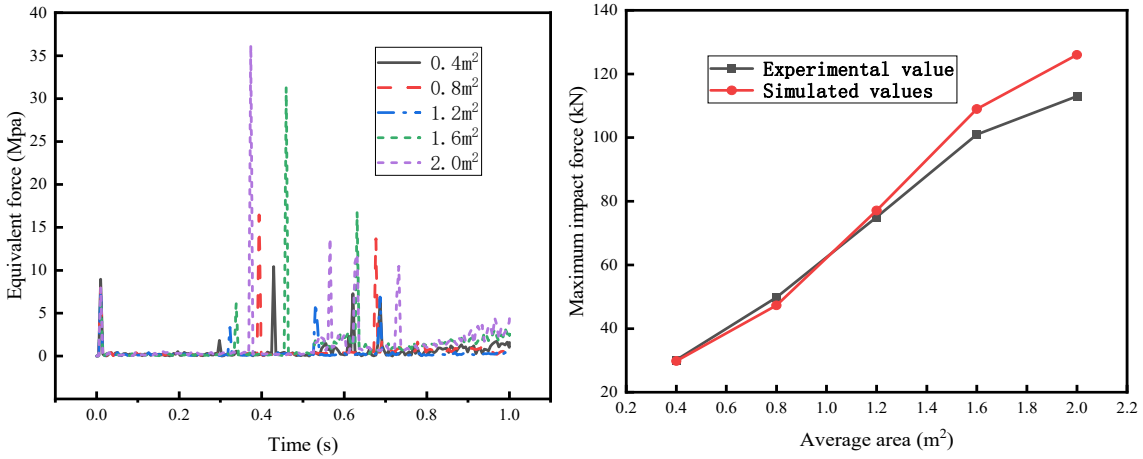

(**a**) (**b**)

Figure 17. (**a**) Equivalent stress test data diagram; (**b**) comparison diagram between simulated data and experimental data.

According to the results of comparison between the simulated and experimental values under the four types of area conditions presented in Figure 17b, the results of the impact of different sea-ice areas show a linear trend in general, and with the increase in sea-ice area, the impact force shows an increasing trend, the simulated values of 0.4 m^2 and 0.8 m^2 sea ice are smaller than the experimental values, and according to the on-site observation, it is found that the larger the area of the sea ice, the more pronounced is the 'water cushion effect', and thus the smaller the area of sea ice the higher is the fit of the experimental values with the simulated values, but the error is still within the control. According to the field observation, the larger the sea ice area is, the more obvious the 'water cushion effect' is, and the larger the maximum impact force of the simulated value is, thus, the smaller the sea ice area is, the higher the fit between the experimental value and the simulated value is, and vice versa, thus the lower the fit is, but the error is still within the controllable range. It is concluded that under different average area conditions, the maximum impact force of sea ice hitting the contact area of bridge abutment shows a similar trend with the simulated value. The maximum error is 10.3%, the minimum error is 1.3%, and the average error is 6.38%. By carefully comparing the experimental data with the simulation results, good consistency was found between them, which further proves that the ice material model parameters used for numerical simulation, as well as the simulation results derived from the ALE algorithm, have a certain degree of reliability. These research results contribute to a more in-depth understanding of the effects of small- and medium-sized sea ice on bridge piers and provide important guidance for related engineering practices.

5. Conclusions

Continuous sea ice collision abutment dynamic response research, the application of finite element analysis software ANSYS/LS-DYNA and programming software MATLAB, based on different spacing of sea ice, different average area of sea ice, and sea ice average area conditions simulation of sea ice and railway bridge abutment impact role, through the simulation of the data generated by the analysis of the following conclusions:

(1) Consider the case of different spacing of sea ice: spacing 0.2 m, continuous chain collision is obvious; spacing 0.4 m, the peak value of the secondary collision increases significantly; spacing 0.6 m, sea ice climbing obviously, the secondary peak value is greater than the primary peak value; spacing 0.8 m, is the side of the length of the side of the 0.4 m twice, the subsequent ice extrusion overlap probability increases. Continuous positive collision ice spacing increases, the collision force decreases, and the probability of ice climbing and overturning increases. The stability of the bridge abutment is most affected in the extrusion phase, and the impact of the subsequent

extrusion increases step by step as the sea ice spacing increases and the collision force decreases, and the probability of sea ice climbing and overturning increases during the successive collision and collision phases. In the subsequent study, different bridge ice contact areas can be investigated under the influence of ice spacing.

(2) With the increase of sea ice mass, i.e., average area and thickness, the impact force on the bridge abutment increases step by step. In the initial collision stage, the peak impact force increases linearly with the increase of sea ice area and thickness, and the maximum impact force is 125.94 kN and 66.86 kN, respectively. In the crush collision stage, the distribution of the equivalent force of the bridge abutment is mainly on the side of the contact neighboring area. The climbing and overturning phenomenon of sea ice is more obvious with the increase of thickness; the stability of the bridge abutment is mainly in the first collision stage; there is a risk of impact instability; the second peak of the successive positive collision is higher; and the effect of mass on the impact of sea ice on the bridge abutment is more significant than the acceleration, so the subsequent research process needs to be set up for the stage of the collision of different shapes of collision avoidance bodies and study the advantages and disadvantages of the study.

(3) In the case of collision of different shapes of sea ice, the maximum value of impact force appears in the first collision stage as the average area of sea ice increases, and the subsequent sea ice shows an obvious climbing phenomenon and enters the extrusion stage. The average area of sea ice is larger than 1.5 m^2 with higher quality, and the maximum impact force is 182.8 kN, which is obvious to the bridge abutment. With the increase of the average area of sea ice, the maximum impact force on the bridge abutment increases step by step, and the experimental and simulated values of the maximum impact force of sea ice hitting the contact area of the bridge abutment show a similar trend. The larger sea ice in the irregular sea-ice layer causes a larger impact force, and the phenomenon of accumulation and climbing occurs, squeezing around the bridge abutment, increasing the impact force of the water flow on the bridge abutment, leading to an increase in the instability of the bridge abutment structure. In the subsequent study, only sea ice with an average area of 1.5 m^2 is studied, and different two-dimensional cutting surfaces are investigated and analyzed.

(4) Based on the design of the experimental program to study only the impact of sea ice area on the concrete structure of the bridge pier, under different area conditions, the maximum impact force of sea ice impact on the contact area of the bridge pier experimental values and simulated values show an increasing trend. The maximum error is 10.3%, the minimum error is 2.7%, and the average error is 7.65%. There is good consistency between the experimental value and the simulated value, which proves that the parameters of the ice material model used for numerical simulation and the simulation results of the area data based on the Voronoi cutting algorithm have a certain degree of reliability.

Author Contributions: L.G.: methodology, software, investigation, data curation, funding acquisition, writing—original draft, visualization. Y.C.: methodology, supervision, validation, resources, writing—review and editing. Y.D.: conceptualization, methodology, supervision, validation, resources, writing—review and editing. L.Q.: methodology, supervision, resources, writing—review and editing. X.Z.: methodology, software, supervision, writing—review and editing. All authors have read and agreed to the published version of the manuscript.

Funding: This study was the financially supported by the National Science Foundation (72261024, 51969011) of China; Gansu Provincial Science and Technology Programme Grant (23ZDFA002), Gansu Provincial Key Talent Project (2023RCXM27); Gansu Provincial Department of Education Higher Education Industry Support Programme Project (2022CYZC-32); Gansu Provincial Department of Transportation and Communication Science and Technology Project (2022-27).

Data Availability Statement: All data included in this study are available upon request by contacting the corresponding author.

Conflicts of Interest: The authors declare no conflicts of interest.

References

1. Song, W.D.; Ning, J.U. Critical force of ice on marine structures. *Glacial Permafr.* **2003**, *03*, 351–354.
2. Qu, Y. *Random Ice Load Analysis of Marine Structures Based on Field Experiments*; Dalian University of Technology: Dalian, China, 2006.
3. Lemström, I.; Polojärvi, A.; Tuhkuri, J. Modelscale tests on ice-structure interaction in shallow water: Global ice loads and the ice loading process. *Mar. Struct.* **2022**, *81*, 103106. [CrossRef]
4. Metrikin, I.; Kerkent, S.; Jochmann, P.; Løset, S. Experimental and numerical investigation of dynamic positioning in level ice. *J. Offshore Mech. Arct. Eng.* **2015**, *137*, 031501. [CrossRef]
5. Gong, L.; Dong, Z.Q.; Yang, T.T. Dynamic response analysis of ice-pier collision in Water. *J. Vib. Shock* **2024**, *43*, 72–82.
6. Zhu, L.; Cai, W.; Chen, M.; Tian, Y.; Bi, L. Experimental and numerical analyses of elastic-plastic responses of ship plates under ice floe impacts. *Ocean Eng.* **2020**, *218*, 108174. [CrossRef]
7. Zhang, J.M.; Yuan, Z.G.; Wu, Y.P. Analysis on the collision couple between drift ice and long-span prestressed concrete T-rigid frame bridge pier. In *Key Engineering Materials*; Trans Tech Publications Ltd.: Wollerau, Switzerland, 2015; Volume 648, pp. 17–24.
8. Wu, T.; Qiu, W. Dynamic analyses of pile-supported bridges including soil-structure interaction under stochastic ice loads. *Soil Dyn. Earthq. Eng.* **2020**, *128*, 105879. [CrossRef]
9. Xia, C.Y.; Lei, J.Q.; Zhang, N. Analysis of Dynamic Response and Train Operation Safety of high-speed Railway Bridge under Impact Load. *Eng. Mech.* **2012**, *29*, 101–107+120.
10. Li, P.; Li, Z.; Han, Z.; Zhu, S.; Zhai, W.; Lou, H. Running safety evaluation of high-speed train subject to the impact of floating ice collision on bridge piers. *Proc. Inst. Mech. Eng. Part F J. Rail Rapid Transit* **2022**, *236*, 220–233. [CrossRef]
11. Wang, B.; Yu, H.C.; Basu, R. Ship and ice collision modeling and strength evaluation of LNG ship structure. In Proceedings of the ASME 2008 27th International Conference on Offshore Mechanics and Arctic Engineering: American Society of Mechanical Engineers, Estoril, Portugal, 15–20 June 2008; pp. 911–918.
12. Kawano, Y.; Ohashi, T. Numerical study on c-axis orientations of sea ice surface grown under calm sea conditions using a particle method and Voronoi dynamics. *Cold Reg. Sci. Technol.* **2015**, *112*, 29–38. [CrossRef]
13. Liu, L.; Long, X.; Ji, S.Y. Discrete element method based on extended polyhedron and its ice load calculation on round pile. *Chin. J. Mech. Mech.* **2015**, *47*, 1046–1057.
14. Guo, Y.K.; Han, X.Y.; Meng, W.Y. Finite element analysis of pier safety under flow ice Collision. *J. North China Inst. Water Resour. Hydropower* **2013**, *34*, 16–18.
15. Yang, L.; Ma, J. Numerical Simulation analysis of collision between ship and offshore platform under ice medium. *China Offshore Platf.* **2008**, *23*, 29–33.
16. Gong, L.; Dong, Z.; Jin, C.; Jia, Z.; Yang, T. Flow–Solid Coupling Analysis of Ice–Concrete Collision Nonlinear Problems in the Yellow River Basin. *Water* **2023**, *15*, 643. [CrossRef]
17. Hu, Y.D.; Guo, W.N.; Zhang, Y. Analysis on the evolution of transit in the Ningzhou-Mongolia Reach of the Yellow River from 2011 to 2020. *Yellow River People* **2023**, *45*, 52–57.
18. Wang, E.L.; Hu, S.B.; Han, H.W. Study on flow density of Kaijiang River in Heilongjiang Province based on UAVS low altitude remote sensing and OTSU algorithm. *J. Hydraul. Eng.* **2019**, *53*, 68–77.
19. Yu, Y.W. *Numerical Simulation of Ship-Ice Collision in Ice Breaking Area*; Dalian University of Technology: Dalian, China, 2022.
20. Chen, Y.F. *Study on the Evolution Mechanism of ICE Transport and Its Application in Two-Phase Outwash Flow Channel*; China Institute of Water Resources and Hydropower Research: Beijing, China, 2019.
21. Zhu, H.R.; Ji, S.Y.; Liu, L. Structure and discrete element analysis of ice fragmentation region based on Voronoi cutting algorithm. *Chin. J. Comput. Mech.* **2019**, *36*, 454–463. (In Chinese)